Attributing hypoxia responses of early life *Menidia menidia* to energetic mechanisms with Dynamic Energy Budget theory

Teresa G. Schwemmer [a,*], Roger M. Nisbet [b], Janet A. Nye [c]

[a] *School of Marine and Atmospheric Sciences, Stony Brook University, Stony Brook, NY 11794, USA*
[b] *Department of Ecology, Evolution and Marine Biology, University of California Santa Barbara, Santa Barbara, CA 93106, USA*
[c] *Department of Earth, Marine and Environmental Sciences, University of North Carolina at Chapel Hill, Institute of Marine Sciences, Morehead City, NC 28557, USA*

ARTICLE INFO

ABSTRACT

Ocean deoxygenation is intensifying worldwide due to warming and eutrophication, particularly in estuaries and coastal waters. Although the Atlantic silverside (*Menidia menidia*) is tolerant of the fluctuating environmental conditions in its estuarine habitat, chronic hypoxia impairs hatching, growth, and survival in the early life stages. We used a simplified version of a Dynamic Energy Budget model (DEBkiss) to test the hypothesis that experimentally observed changes in animal performance can be explained by one or more of the rate processes in the model. We sought to identify the DEBkiss parameters that, when adjusted with a correction factor based on inhibition of Synthesizing Units, provided the best fit to hypoxia effects in the three state variables of total length, egg buffer mass, and survival over time. Because hypoxia reduces survival in embryos and newly hatched larvae, we added a survival state variable controlled by pre- and post-hatching mortality parameters. Applying the hypoxia effects to reduce the conversion efficiency of assimilates to structure accounted for some of the hypoxia-related changes in all three state variables. However, the best fit was achieved by simultaneously reducing the conversion efficiency and increasing both mortality parameters. In contrast, changing the parameter for maintenance rate with hypoxia provided little to no improvement of fit to the data. Reduced conversion efficiency under hypoxia would suggest that less of the energy invested by parents and consumed through predation is converted into biomass in *M. menidia* offspring, with implications for size at age that could threaten recruitment and alter the flow of energy through the food web.

1. Introduction

Hypoxia is common in coastal and estuarine waters and is expected to intensify with global warming (Diaz and Rosenberg, 2008; Breitburg et al., 2018). Between anthropogenic influence on nearshore waters and the natural dynamics of shallow, partially enclosed water bodies, hypoxia often co-occurs with other stressors such as high temperature, ocean acidification, and pollutants (Gruber, 2011). In temperate estuaries, stratification and productivity associated with high temperatures in spring and summer cause hypoxic and eutrophic zones to form with great fluctuations in dissolved oxygen (DO) on diel to monthly time scales (O'Donnell et al., 2008; Baumann and Smith, 2018; Testa et al., 2018). While fish species that currently live in such areas tend to have mechanisms to cope with episodic hypoxia (Farrell and Brauner, 2009; Zhu et al., 2013; Baumann, 2019), these are not necessarily adequate for tolerance of longer duration events. Fishes that spawn in the spring and

summer may be particularly vulnerable because they are exposed to hypoxia during the sensitive early life stages. Embryos and young larvae rely largely on diffusion for oxygen uptake and lack well-developed mechanisms, such as high surface area gills, to meet oxygen demands in low DO water (Rombough, 1988). While later stage fishes and even some early larvae can swim to avoid hypoxic habitats (Niklitschek and Secor, 2005; Chapman and McKenzie, 2009), embryos cannot utilize this response. Mortality can result directly from severe hypoxia or indirectly from reduced growth increasing susceptibility to predation. Even fish that survive may incur sublethal effects with lasting, lifelong consequences for growth, development, and reproduction (Stierhoff et al., 2006; Vanderplancke et al., 2015; Zambonino-Infante et al., 2017). Modeling the energetic mechanisms of responses to hypoxia using unified principles on model species can help connect physiology and life history to population-level changes and serve as a valuable alternative and/or supplement to time- and labor-intensive laboratory experiments

---

on other species, particularly with very small embryos and larvae.

Hypoxia is known to inhibit growth and survival in early life fishes (Rombough, 1988; Cross et al., 2019; Del Rio et al., 2019), as oxygen is required for the processes that maintain homeostasis and convert food for growth and activity. Anaerobic energy production fuels these processes with only about 1/15th the ATP yield of aerobic respiration. Hypoxic exposure may lead to physiological responses such as depressed metabolism (Richards, 2009; Schwemmer, 2023), limited growth, increased ventilation, and changes to hematocrit, hemoglobin, and erythrocyte quantities and characteristics (Taylor and Miller, 2001; Stierhoff et al., 2009; Bianchini and Wright, 2013). Metabolism has also been shown to increase after temporary hypoxia as fish remove lactate accumulated from anaerobic respiration (Heath and Pritchard, 1965). While the growth and survival effects of hypoxia have been demonstrated in many species, the mechanisms are poorly understood. The Atlantic silverside (*Menidia menidia*) is an estuarine forage fish that has frequently been used as a model species to understand effects of stressors, including hypoxia, on fish growth and physiology (DePasquale et al., 2015; Miller et al., 2016; Schwemmer et al., 2020). Hypoxia significantly delays *M. menidia* hatching and reduces embryo and larval growth (Cross et al., 2019).

Dynamic Energy Budget (DEB) theory is a bioenergetic framework designed to bridge multiple levels of biological organization in assessing stressor effects and their mechanisms in a vast variety of species (Kooijman, 2010a; AmP, 2023). This approach follows energy allocation, represented in suborganismal metabolic fluxes, and how it leads to life history outcomes such as growth rate, reproductive output, and survival, using physical and biological concepts that are generalizable to most species (Jusup et al., 2017). It accounts for differences in the energy budget at each stage to allow modeling of life stage transition timing and stage-specific responses to stressors (Kooijman, 2010a). DEB theory is often used to connect experimental observations of multiple stressor effects to both the underlying energetic mechanisms (Kooijman, 2018) and life history outcomes that feed into population dynamics (Nisbet et al., 2000; Martin et al., 2013; Smallegange et al., 2017). It is important to connect suborganismal and organismal responses to population implications because targeted conservation actions typically operate at this level, but this scaling requires additional steps and remains a challenge (but see Nisbet et al., 1989; Martin et al., 2013; Grear et al., 2020; Tai et al., 2021). The ability to bridge levels of biological organization from the molecular to population level makes DEB theory an excellent tool for enhancing the utility of experimental hypoxia data

for conservation and management (Lavaud et al., 2021). However, there is a conceptual disconnect between the abstract variables and fluxes in DEB models and the chemically defined quantities reported in most molecular-level studies (e.g. Murphy et al., 2018). Some of the interpretation of our results in this paper rests on hypothesized connections between these different levels of description, and for this reason we discuss some suborganismal literature in detail in the Supplementary Materials, section *Relating DEB processes to physiology*.

Depending on the application and types of data available, simplified versions of the standard DEB model can be used (e.g. Kooijman and Metz, 1984; Jager, 2018; Martin et al., 2017). Although complexity can sometimes be beneficial (Evans et al., 2013), simple parameter-sparse models are often preferable for their predictive power and ability to be applied, tested, and interpreted widely (Holling, 1966; Jusup et al., 2017). The DEBkiss framework (Fig. 1) is a moderately simplified variation on the standard DEB model for animals that eliminates explicit representation of reserve and assumes that assimilates are immediately allocated to structure, maintenance, and reproduction (Jager et al., 2013). This reduces the data requirements and, depending on the data, the total number of parameters to be estimated (Jager et al., 2013). The simplicity of DEBkiss makes it ideal for adaptation to many species of ecological or commercial value, even when the existing studies were not originally intended for this use. Romoli et al. (2024) present a detailed comparison of the advantages and limitations for ecological risk assessment of a model based on DEBkiss versus a model based on Kooijman's "standard" DEB model. They highlight several "modeling choices" that should influence the choice of approach, including: (i) insufficient information in data sets; (ii) capturing differences between data sets for the same species; and (iii) auxiliary hypotheses. Consideration of each of these led us to choose DEBkiss for our work after much unsuccessful effort attempting to interpret parameter estimates with the standard model (using the Add-my-Pet software; AmPtool, 2022; Marques et al., 2018).

We used DEBkiss to test the hypothesis that changes in animal performance under hypoxia can be explained by changes in one or more of the rate processes in the model, and to identify the bioenergetic mechanisms underlying experimental hatching, growth, and survival effects of hypoxia in early life stages of *M. menidia* observed in Cross et al. (2019). First, we fit the DEBkiss model to full-life data on total length, reproductive output, hatch timing, and survival and estimated or calculated parameters under fully oxygenated conditions. Second, we used the concept of Synthesizing Units (SU) that are inhibited or
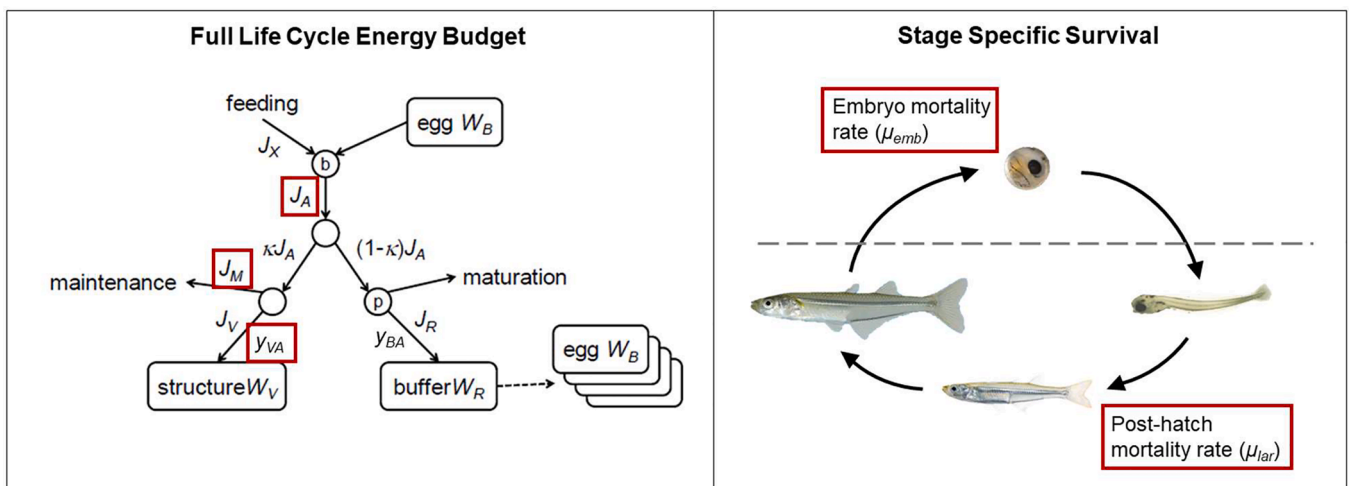

Fig. 1. Conceptual diagram of the DEBkiss model highlighting parameters of interest for hypoxia effects. The DEBkiss model (diagram adapted from Jager et al., 2013) used in this study includes stage-specific survival parameters. The hypothesized parameters for hypoxia stress mechanisms are highlighted in red boxes. The left panel shows the energy budget for the full life cycle and the right panel shows how the stage-specific survival modification is applied to embryos, larvae, juveniles, and adults of *M. menidia*.

damaged by hypoxia to directly or indirectly change key parameters in the DEBkiss model (Muller et al. 2019). SUs are generalized enzymes that produce products such as body structure or support maintenance requirements from incoming fluxes of substrate, i.e. food or egg buffer (Kooijman, 1998, 2010a). With single substrates for each life stage the SU formalism is equivalent to standard Michaelis-Menten kinetics, but the SU interpretation allowed us to exploit the subtleties in describing inhibition set out by Muller et al. (2019). We used a correction factor based on inhibition or damage to the SU to fit the model to early-life data for four DO treatments. We evaluated which parameter or combination of parameters, when adjusted with the correction factor, was able to best account for the full set of hypoxia responses observed in experiments and thus allow inference of mechanism.

2. Methods

2.1. DEBkiss model description

The material flows are shown in Fig. 1. The yolk in an egg is treated as a buffer of "food" for the developing embryo that initially has an infinitesimally small structural biomass. In this regard, DEBkiss differs from standard DEB where the yolk is considered to be "reserve" whose dynamics are treated similarly to that for feeding life stages. There is no reserve compartment between food assimilation and its utilization. Birth occurs when the egg buffer is fully depleted. After birth, larvae and juveniles, which are treated identically in this model, feed and assimilated food is allocated to growth, maturation, and both somatic and maturity maintenance in accordance with the κ-rule. After reaching puberty and entering the adult stage, individuals feed and reproduce while maturation ceases. Somatic and maturity maintenance continue in adults.

The DEBkiss assumptions and equations are from Jager (2018). The parameters are defined in Table 1 and the variables, differential equations, and conversions are defined in Table 2. The flux of food or, for embryos, from the egg buffer (W_B) is immediately converted to assimilates which are allocated to a somatic fraction (κ) and a reproductive fraction ($1-\kappa$; Fig. 1). The assimilation flux (J_A) is the product of the scaled measure of resource availability (f), the volumetric surface area (L^2), and the parameter maximum area-specific assimilation rate (J_{Am}^a) where $f = 1$ for embryos and for post-hatching fish fed *ad libitum*. Within the somatic branch, a flux to maintenance (J_M) is prioritized while the remainder goes to structural mass (J_V) with a conversion efficiency y_{VA}. The maintenance flux is proportional to structure.

For larvae and juveniles, the non-somatic fraction of assimilates is spent on maturation, or increasing complexity, through which it is dissipated and does not contribute to biomass. While the standard DEB

Table 1
DEBkiss parameters, their abbreviations, and their fixed or estimated values from fitting to full life data. Units are given with the value unless the parameter is a unitless ratio. All masses are in mg of dry weight.

Parameter	Symbol	Fixed or estimated	Value
Max. area-specific assimilation rate	J_{Am}^a	Estimated	0.333 mg mm^{-2} d^{-1}
Max. volume-specific maintenance rate	J_M^v	Fixed	0.0214 mg mm^{-3} d^{-1}
Initial egg buffer mass	W_{B0}	Fixed	0.15 mg
Total physical length at puberty	L_p^M	Fixed	102 mm
Yield of assimilates on structure	y_{AV}	Fixed	0.8
Yield of egg buffer on assimilates	y_{BA}	Fixed	0.95
Conversion efficiency of assimilates to structure	y_{VA}	Estimated	0.365
Fraction of assimilates allocated to soma	κ	Fixed	0.8
Scaled food level	f	Fixed	1
Scaled food level for embryo	f_B	Fixed	1
Embryo mortality rate	μ_{emb}	Estimated	0.0639 d^{-1}
Post-hatch mortality rate	μ_{lar}	Estimated	0.0294 d^{-1}

Table 2
Model definition. Fluxes, state variables, and differential equations in the DEBkiss model.

Flux	Symbol	Equation	Units
Assimilation flux	J_A	$J_A = f\,J_{Am}^a\,L^2$	mg day^{-1}
Maintenance flux	J_M	$J_M = J_M^v\,L^3$	mg day^{-1}
Flux to structural growth	J_V	$J_V = y_{VA}\,(\kappa\,J_A - J_M)$	mg day^{-1}
Flux to reproduction buffer	J_R	$J_R = (1-\kappa)\,J_A - J_J$ when $W_V \geq W_{Vp}$	mg day^{-1}
		$J_R = 0$ when $W_V < W_{Vp}$	
Flux to maturity maintenance	J_J	$J_J = J_J^v L^3$ when $W_V < W_{Vp}$	mg day^{-1}
		$J_J = J_J^v \dfrac{W_{Vp}}{d_V}$ when $W_V \geq W_{Vp}$	

State Variable	Symbol	Equation	Units
Structural dry mass	W_V	$\dfrac{dW_V}{dt} = J_V$	mg day^{-1}
Continuous reproduction rate	R	$\dfrac{dR}{dt} = \dfrac{y_{BA}\,J_R}{W_{B0}}$	eggs day^{-1}
Egg buffer (yolk) mass	W_B	$\dfrac{dW_B}{dt} = -J_A$	mg day^{-1}
Survival	S	$\dfrac{dS}{dt} = -\mu_{emb}\,S$ when $W_B > 0$	day^{-1}
		$\dfrac{dS}{dt} = -\mu_{lar}\,S$ when $W_B = 0$	

Other variables and conversions	Symbol	Equation	Units
Total physical length	L^M	$L^M = \dfrac{L}{\delta_M}$	mm
Volumetric length	L	$L = \delta_M L^M = \sqrt[3]{\dfrac{W_V}{d_V}}$	mm
Shape coefficient	δ_M	$\delta_M = \dfrac{L}{L^M}$	unitless
Dry weight density of structure	d_V	$d_V = \dfrac{W_V}{L^3}$	mg mm^{-3}
Dry mass at puberty	W_{Vp}	$W_{Vp} = d_V * (L_{Vp} * \delta_M)^3$	mg
Volume-specific maturity maintenance costs	J_J^v	$J_J^v = \dfrac{1-\kappa}{\kappa} * J_M^v$	mg mm^{-3} day^{-1}
Scaled measure of resource availability	f	–	unitless (range 0–1)

formulation uses a state variable for maturity that triggers changes between life stages, DEBkiss instead uses a constant size at puberty to specify when reproduction is initiated (Kooijman, 2010b; Jager et al., 2013), so the maturity variable plays no role in the current work. Once the mass at puberty is reached (W_{Vp}), reproductive flux (J_R) toward egg production begins in adults with a conversion efficiency y_{BA}. The flux to maturity maintenance (J_J) is the product of the volume-specific maintenance costs (J_J^v) and structural volume, or the volume at puberty for adults. J_J^v is calculated from κ and J_M^v (Table 2), rather than estimated, as connecting the two maintenance costs allows cumulative investment in maturity at puberty to be independent of food level (Jager, 2018).

Starvation is defined in two stages, with the first stage being insufficient flux of assimilates to the somatic fraction to meet maintenance requirements so that energy is diverted from the flux to maturation or the reproduction buffer. In the second stage, when the flux to both the somatic and reproductive branches is insufficient and the reproduction buffer is empty or puberty has not been reached, structure is converted to assimilates with conversion efficiency y_{AV} to go towards maintenance costs (Jager, 2018).

Because our growth data are in total length, we used a shape correction coefficient (δ_M) and dry weight density (d_V) to connect length with the model state variables (Table 2). δ_M connects the total length (L^M) to the volumetric length (L) which is the cubic root of volume, and d_V connects volume to structural dry mass. δ_M could plausibly have different values in different life stages (section 7.8 of Kooijman, 2010a), but lacking relevant data we here assume a single stage-independent value. We calculated these constants using data on *M. menidia* length (Klahre, 1997) and embryo volume (Schwemmer, unpublished data; methods in Supplementary Materials) and a total length (L^M) to dry weight (W_V) conversion empirically derived from data on larval to adult

stages (Concannon et al., 2021):

$$W_V = 0.0012 * L^{M\ 2.997} \tag{1}$$

After calculating W_V from $L^M = 5.3$ mm at hatching (Cross et al., 2019), we obtained a dry weight at hatching of 0.18 mg. Assuming there is negligible change in weight or volume during hatching, we used the volume of an embryo immediately before hatching, $L^3 = 0.45$ mm^3, to calculate d_V using:

$$d_V = \frac{W_V}{L^3} \tag{2}$$

This gave us $d_V = 0.4$ mg mm^{-3}. This is slightly higher than the d_V values used for other fish species (e.g. Jager et al., 2022), but the overall results were not sensitive to this parameter and it allowed for a good fit to growth data across all life stages. More details on this calculation can be found in the Supplementary Materials. We similarly used the embryo volume to calculate volumetric length of an embryo as $L = 0.77$ mm, which gives us a δ_M of 0.145 using the following equation:

$$\delta_M = \frac{L}{L^M} \tag{3}$$

However, this value led the model to underestimate total length later in the life span, suggesting the δ_M value was too high for this long and slender fish. This underestimation indicates that the shape of a newly hatched larva is not representative of the shape throughout life and after feeding begins, and this conversion could be refined for future work by making volume and length measurements at multiple life stages to implement stage-specific δ_M values. We manually adjusted δ_M to a final value of 0.107 which provided a reasonable fit to length data and a better starting point for parameter estimation.

We added a survival state variable (S) which, in addition to allowing an alternative outcome to hatching, enabled us to model survival as a consequence of hypoxia effects on the energy budget. We fit mortality parameters for embryos and post-hatch fish (μ_{emb} and μ_{lar}) to data for survival to hatching and larval/juvenile survival (Fig. 1; Table 2). In our implementation of survival, the only DEB process influencing survival is egg buffer depletion, which determines the time to hatch and thus when the embryo mortality rate switches to the post-hatch mortality rate. This means survival is indirectly affected by the assimilation rate and conversion efficiency of assimilates into structure.

2.2. Data

We calculated and estimated DEBkiss parameters in normoxic conditions (Section 2.3) and modeled hypoxia effects (Section 2.5) based on four types of data: total length over time, egg buffer mass over time (initial egg mass and age at hatching when egg buffer mass is assumed to be zero), cumulative egg production over time, and proportion surviving since fertilization over time. As described in the introduction, the data available for this model led us to use DEBkiss over the "standard" DEB model based on the factors highlighted by Romoli et al. (2024) and unsuccessful attempts to use standard DEB. We had insufficient data, had to integrate information from multiple studies of the same (and similar) species, and had to hypothesize plausible values for a few parameters.

Data for total length were sourced from four studies. Length at hatching and 15 days post-hatching (dph) came from a study that reared *M. menidia* offspring in different static oxygen levels across two experiments (Cross et al., 2019). This provided data for parameter estimation at control oxygen levels described in Section 2.3 and modeling three reduced oxygen treatments (Section 2.5 and Table 2). We sourced additional length data for the full life span from control levels of experiments that exposed *M. menidia* offspring to ambient and elevated CO$_2$ levels (Murray and Baumann, 2018; 2020; Concannon et al., 2021). All total length data were obtained from fish maintained in static laboratory conditions at 24 °C.

Data for the state variables of egg buffer mass (via time to hatching, when egg buffer mass is zero), as well as survival at hatching and at 15 dph, were obtained from Cross et al. (2019). Because *M. menidia* hatch with little to no yolk sac (Bayliff, 1950; Bigelow and Schroeder, 1953) and begin feeding the day of hatching (Middaugh and Lempesis, 1976), we equate hatching with birth and assume the egg buffer mass reaches zero at hatching. The hatch timing data use time steps of 1 day, so any very short delay between hatching and the start of feeding would not be reflected in the model. The control data from these experiments were used to estimate parameters under normoxia (Section 2.3). We also obtained normoxic survival data from a study on the effects of temperature and CO$_2$ on *M. menidia* early life survival, using only the 24 °C and control CO$_2$ data (Murray and Baumann, 2018). Four additional data points for long-term survival in laboratory conditions at 17 °C were obtained from a study that exposed *M. menidia* offspring until 122 dph to two CO$_2$ levels, of which we only used data from the control level (Murray et al., 2017). Lastly, the data for cumulative egg production over time, used to estimate parameters under normoxia (Section 2.3), were also obtained from control groups in Concannon et al. (2021), a study in which wild-caught juveniles were held in the laboratory at 20 °C in different CO$_2$ treatments and strip-spawned once they reached reproductive maturity.

2.3. Parameter estimation under normoxia

We estimated four parameters by fitting them to full-lifespan data listed in Section 2.2 (J_{Am}^a, y_{VA}, μ_{emb}, and μ_{lar}), calculated four parameters from data (J_M^y, W_{B0}, L_p^M, and f), and fixed at suggested values parameters for which we had insufficient data to calculate or estimate (y_{AV}, y_{BA}, κ, and f_B; Jager, 2018). The primary parameters and their calculated or estimated values are found in Table 1. Fitting was done in Matlab with the platform BYOM v.6.4 and the package DEBkiss v.2.3a (https://www.debtox.info/byom.html). Details on parameter estimation in BYOM can be found in the Supplementary Materials.

We were able to obtain a reasonable fit using suggested values for y_{AV}, y_{BA}, and κ for unstressed fish that are thought to be widely applicable across species (Lika et al., 2011; Jager, 2018). We used length, reproduction, and egg buffer depletion data to estimate y_{VA} with the BYOM optimization. Ultimate length was used to fit J_{Am}^a to a reasonable value while fixing all other parameters before estimating y_{VA}, because both parameters affect growth and egg buffer depletion in the model and therefore cannot be estimated simultaneously. Finally, we used the BYOM optimization to estimate μ_{emb} and μ_{lar}.

The length and reproductive data allowed us to calculate "length at puberty" (L_p^M), defined as the length at which egg production begins. We obtained W_{B0} from *M. menidia* egg dry weight data (Klahre, 1997) and calculated δ_M and d_V from total length, egg diameter, and egg mass data (Cross et al., 2019; Klahre, 1997; Concannon et al., 2021). To calculate volume-specific maintenance costs (J_M^y), we used data on the rate of decrease in larval dry weight over a period of starvation in the congeneric species *M. beryllina* (Letcher and Bengtson, 1993). More detail on this calculation can be found in the Supplementary Materials. Borrowing from closely related species is a common practice in bioenergetic modeling when the species has similar habitat, life history, and physiology (Sibly et al., 2013). *M. menidia* and *M. beryllina* have overlapping habitats and similar life history, egg sizes, and body sizes, although *M. beryllina* reaches a smaller ultimate length (Middaugh, 1981; Bengtson, 1984; Middaugh and Hemmer, 1992). All *M. menidia* experiments used in this study fed fish *ad libitum* in all treatment levels, so f was set to 1. For studies that exposed fish to different CO$_2$ levels, we only used data from control groups to avoid potential CO$_2$ effects in the data.

2.4. Relating DEB processes to physiology

We aimed to identify the DEBkiss parameters responsible for observed whole-organism effects of rearing *M. menidia* in hypoxia by

applying a correction factor to modify one or more parameters with decreasing oxygen based on inhibition of or damage to a SU. The SU controls assimilation, the transformation of food (or yolk) and oxygen into compounds that will go to structure, maintenance, or reproduction (Kooijman, 2010a; Jager, 2018). Although oxygen can be a limiting substrate in SUs, previous work suggests that *M. menidia* embryos only become metabolically oxygen-limited below a critical level of 2.04 mg L^{-1} (Schwemmer, 2023), while it remains oxygen-independent at the treatments for which we have data (2.7, 3.1, 4.2, and 7.7 mg L^{-1}; Schwemmer et al., 2020). We therefore considered a single-substrate growth SU in which food or egg buffer was the substrate. The mathematical characterization of inhibition and damage is in Section 2.5.

Inhibiting agents reversibly bind to SUs, preventing them from accepting substrates to proceed with their reaction. Damage, in contrast, induces dysfunction that is irreversible upon removal of the damaging agent; however, damaged SUs can be repaired or replaced (Muller et al., 2019). The idea is that hypoxia induces the production of compounds that in turn bind to SUs. We used existing information on the physiological responses of fish early life stages to hypoxia to identify the following candidate DEBkiss parameters to which to apply the hypoxia-based correction factor: maximum assimilation rate (J_{Am}^a), conversion efficiency of assimilates into structure (growth, y_{VA}), maximum somatic maintenance rate (J_M^y, mg mm^{-3} d^{-1}), embryo mortality rate (μ_{emb}), and post-hatch mortality rate (μ_{lar}). Hypoxia effects on growth and hatching time can occur either through inhibition of assimilation or through damage that reduces the conversion efficiency of assimilates to growth. Hypoxia may impact survival directly through damage or by inhibition of damage repair processes. Hypoxia's impact on somatic maintenance rate may be most plausibly represented as damage. Inhibition of or damage to SUs could affect these parameters as a direct or indirect result of several hypoxia responses in fish, such as anaerobic respiration, behavior, and action of hypoxia-inducible factors (Farrell and Brauner, 2009). A detailed review of how these mechanisms relate to the DEB parameters and SUs can be found in the Supplementary Materials.

2.5. Hypoxia effects

We tested the hypothesis that changes in *M. menidia* early life growth, hatch timing, and survival under reduced oxygen (Cross et al., 2019) can be explained by inhibition or damage linked to one or more DEBkiss processes (Fig. 1). To summarize the experimental data on static hypoxia effects we are attempting to explain by altering these parameters, the mean values of data for each oxygen treatment are listed in Table 3. We used the parameter values from the model fit to full life data and altered one or more parameters at a time with oxygen-dependent correction factors, then fit the model to data for only the first 136 days by estimating a parameter that controls the correction factor's relationship with DO. We only used early life data to fit the hypoxia-altered parameters because we did not have late-life or reproductive data for multiple oxygen treatments against which to validate

Table 3
Summary of experimental data for each DO level. The mean survival to hatching, hatch time (at which egg buffer is zero), length at hatching, length at 15 dph, and survival to 15 dph from the different DO treatments in Cross et al. (2019). The control DO level means (7.7 mg L^{-1}) also include data from Murray and Baumann (2018).

Variable	7.7 mg L^{-1}	4.2 mg L^{-1}	3.1 mg L^{-1}	2.7 mg L^{-1}
Survival to hatching	74.3 %	70.6 %	85.8 %	30.2 %
Hatch time (egg buffer mass = 0)	6 days	7 days	8 days	9 days
Length at hatching	5.3 mm	4.6 mm	4.4 mm	4.1 mm
Larval length at 15 dph	15.8 mm	12.2 mm	9.2 mm	–
Larval survival to 15 dph	44.0 %	22.2 %	20.9 %	0 %

observed changes. It did not make sense to include later life data in the calculations of NLL that influence the parameter estimates or to speculate about how well the predicted data match what we might expect to happen later in life if we not only lack late-life hypoxia data but also do not expect full-life hypoxia to occur in nature.

We derived a correction factor for *inhibition* using the framework developed by Muller et al. (2019), in which inhibitors can act on SU dynamics in five different ways. Out of these, *noncompetitive inhibition* is well-suited to this study because of the limitations of data availability for *M. menidia*. In noncompetitive inhibition the arrival rate of substrate does not affect the binding and dissociation of inhibitors and therefore requires little information about the rate of food uptake (Muller et al., 2019). In this form of inhibition, the rate of assimilation by the SU is:

$$J_A = f J_{Am}^a L^2 \left(\frac{1}{1 + \frac{j_i}{k_i}} \right) \tag{4}$$

where j_i (mg d^{-1}) is the arrival flux of the inhibitor and k_i (mg d^{-1}) is the dissociation parameter. The effect of this relationship in our model is that assimilation declines as the arrival rate of hypoxia-related inhibitors increases. We set j_i to depend on DO treatment above a DO threshold, DO$_c$ (mg L^{-1}), below which j_i is infinitely large, which would bring the rate of the process it is inhibiting to zero:

$$j_i = \begin{cases} \infty & \text{if } DO \leq DO_c \\ \dfrac{1}{B(DO - DO_c)} & \text{if } DO > DO_c \end{cases} \tag{5}$$

B (L $\bullet$ d $\bullet$ mg inhibitor^{-1} $\bullet$ mg O$_2^{-1}$) is a parameter that influences the shape of the relationship between j_i and DO. We defined the correction factor c as the inhibition term (in parentheses in Eq. (4)) and replace j_i with the function from Eq. (5) for DO > DO$_c$ to derive the correction factor c:

$$c = \frac{1}{1 + \frac{1}{k_i B(DO - DO_c)}} \tag{6}$$

As only the product of the parameters k_i and B appear in the formula and we have no need to estimate them separately, they can be combined into one parameter as Z (L mg O$_2^{-1}$). Simplifying Eq. (6) and adding in the case for which DO ≤ DO$_c$ gives us the following correction factor:

$$c = \begin{cases} 0 & \text{if } DO \leq DO_c \\ \dfrac{Z(DO - DO_c)}{1 + Z(DO - DO_c)} & \text{if } DO > DO_c \end{cases} \tag{7}$$

The relationship between c and DO for three different sample values of Z, the parameter to be estimated, is shown in Fig. 2. A larger Z value keeps c higher as oxygen decreases before a more abrupt drop, while a smaller Z gives a more constant decline in c with hypoxia. The value of c cannot exceed 1. DO$_c$ was fixed at a biologically relevant level of 2.04 mg L^{-1}, which is the critical oxygen level below which embryonic routine metabolism becomes highly oxygen-dependent (Schwemmer, 2023). Attempts to estimate DO$_c$ and Z simultaneously showed that leaving DO$_c$ free did not improve the ability of the correction factor to fit the hypoxia data.

Similar simplification of the reasoning by Muller et al. (2019) can be used to derive an analogous correction factor for *damage*. Assuming a proportional change in the rate of damage production to the SU (e.g. via "damage inducing compounds"; Kooijman 2010a), j_d has the same form as Eq. (5). If damage production is quickly balanced by repair or mitigation, then fluxes that decrease through hypoxia will again be reduced by the factor given by Eq. (7). This was recognized by Muller et al. (2019) who noted that if damage production is much slower than the maximum production rate of an SU, the formalism for noncompetitive damage is equivalent to that of noncompetitive inhibition (Muller et al.,
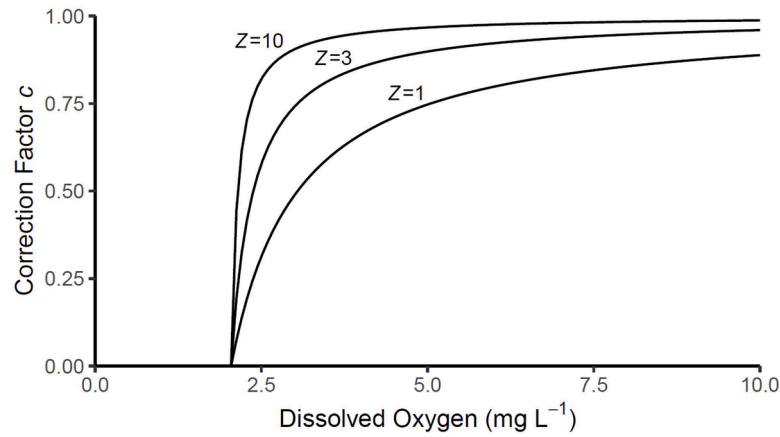
Fig. 2. The correction factor c used to apply hypoxia effects to DEBkiss parameters. The effect of DO on correction factor c is shown at three different values of the parameter Z. Actual estimated Z values are listed in Table 4, and the three Z values used in this figure are sample values to show how Z affects the relationship between DO and c.

2019). Further submodels relating damage to rates that may increase in response to hypoxia (e.g. maintenance and mortality) are needed to derive functional forms for appropriate conversion factors here. Absent information to support such submodels, we hypothesize that the increase was inversely proportional to c defined by Eq. (7).

The correction factor c was multiplied by J_{Am}^a and y_{VA} because these parameters were hypothesized to decrease under hypoxia irrespective of the underlying cause (inhibition or damage). Reductions in the parameter y_{VA} through hypoxia are most plausibly interpreted as damage, the irreversible destruction of functionality of an SU. However, the parameters for maintenance and mortality were divided by c because they were hypothesized to increase, rather than decrease, with damage production and inhibition.

To find the best value of Z for each DEBkiss parameter or combination of parameters, we added Z as a model parameter and estimated it using the BYOM optimization to minimize NLL. We weighted the data equally across treatments to correct for differences in sample size across treatments and prevent one treatment group from disproportionately affecting the estimation of Z, so that all weights within each treatment added up to the same number. We did not apply the correction factor to J_{Am}^a and y_{VA} simultaneously because they both contribute to J_V and their individual contributions to the growth and egg buffer depletion are difficult to disentangle, particularly when J_M is very small as in the early life stages. We only compared the fit of models in which c was applied to parameter(s) that resulted in all three early life datasets – total length, egg buffer mass, and survival – being affected by hypoxia. As a result, either J_{Am}^a or y_{VA} is in each candidate model, because J_M^v, μ_{emb}, and μ_{lar} do not affect egg buffer depletion.

To identify the most likely version of the model (which parameter or combination of parameters best explains the hypoxia effects on the state variables), we estimated Z for each of these scenarios and calculated Akaike's Information Criterion for small sample sizes (AICc). We compared the AICc between each model using the difference between AICc values (ΔAICc) and the relative likelihood of each model using Akaike weights:

$$w_i(AICc) = e^{-0.5 \cdot \Delta_i AICc} \Big/ \sum_{k=1}^{K} e^{-0.5 \cdot \Delta_k AICc}, \tag{8}$$

where $w_i(AICc)$ is the Akaike weight of each model i, $\Delta_i AICc$ is the difference between each model i and the model with the lowest AICc (AICc$_{min}$), and the denominator calculates the sum of relative likelihoods for every model starting at the first model k (Wagenmakers and Farrell, 2004). We used ΔAICc and ratios of Akaike weights to determine which combination of parameters best fit the data when inhibition or

damage was applied and, therefore, which DEB processes best explain the hypoxia effects observed in experiments (Table 4).

3. Results

3.1. DEBkiss model

We obtained realistic fits to the full life cycle data (Fig. 3). The only exception is late-life survival, for which the mortality was too high beyond the larval stage but could not be better fit due to lack of full-life survival data (Fig. 3D). Silversides are an annual species so survival should be greater than 0 % after 150 days. However, this did not impair our ability to model the effects of hypoxia on early life survival, which is most important given that the present study focuses on hypoxia in the early life stages. Estimating y_{VA} returned a value much lower than 0.8, which is the value suggested by Jager (2018) and has been applied in DEBkiss models of other species (e.g. Jager et al., 2018; Hamda et al.,

Table 4
Parameter Z estimates and model selection results. The estimated Z value, AICc, ΔAICc, and Akaike weights when the correction factors were applied to each parameter or combination of parameters. ΔAICc and Akaike weights were calculated with AICc$_{min}$ = 794.03 for the $y_{VA} + \mu_{emb} + \mu_{lar}$ model (bold).

| Parameter(s) affected by hypoxia correction factor	Estimated Z [95 % CI]	AICc	ΔAICc	Akaike weight
J_{Am}^a	3.019 [2.512–3.612]	856.06	62.03	2.5e-14
y_{VA}	1.818 [1.601–2.342]	848.65	54.62	1.0e-12
$J_{Am}^a + J_M^v$	3.105 [2.651–3.726]	855.00	60.97	4.2e-14
$y_{VA} + J_M^v$	1.985 [1.688–2.774]	850.64	56.61	3.7e-13
$J_{Am}^a + \mu_{emb}$	2.804 [1.605–3.287]	823.24	29.21	3.3e-7
$y_{VA} + \mu_{emb}$	1.801 [1.570–2.167]	808.12	14.09	6.3e-4
$J_{Am}^a + \mu_{lar}$	2.930 [2.165–3.428]	838.17	44.14	1.9e-10
$y_{VA} + \mu_{lar}$	1.767 [1.536–2.111]	821.30	27.27	8.7e-7
$J_{Am}^a + \mu_{emb} + \mu_{lar}$	2.819 [1.920–3.286]	810.21	16.18	2.2e-4
$y_{VA} + \mu_{emb} + \mu_{lar}$	**1.827 [1.620–2.269]**	**794.03**	**0**	**0.72**
$J_{Am}^a + J_M^v + \mu_{emb} + \mu_{lar}$	2.913 [2.288, 3.387]	809.96	15.93	2.5e-4
$y_{VA} + J_M^v + \mu_{emb} + \mu_{lar}$	1.981 [1.700, 2.456]	795.97	1.94	0.27
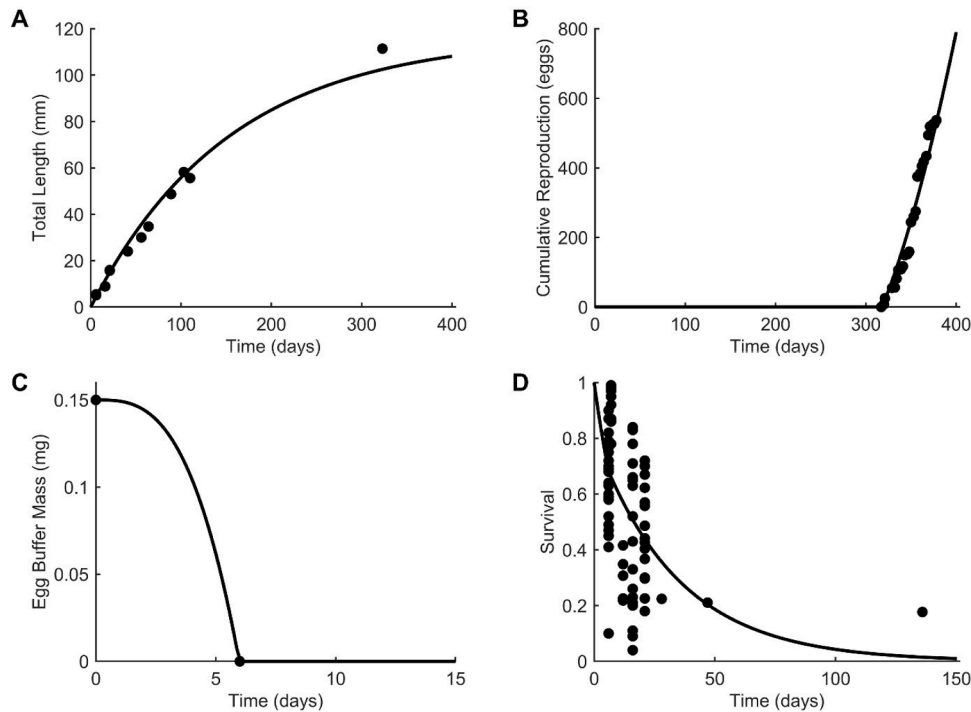
Fig. 3. Full life model fits to data for four state variables. Predicted (lines) and observed data (dots) for the DEBkiss model of *M. menidia* are shown. The state variables are (A) total length (mm) over time (days), (B) cumulative reproduction (eggs) over time (days), (C) egg buffer mass (mg) over time (days), and (D) survival over time (days). Predicted data lines were calculated with the parameter values listed in Table 1.

2019). However, our value of $y_{VA} = 0.365$ is close to the maximum growth efficiency of 0.375 measured in the closely related *M. beryllina* (Letcher and Bengtson, 1993). This gave a realistic fit to the length data and allowed a detailed and very close fit to egg buffer mass over time (hatch timing). The observed and predicted data for full life span are plotted in Fig. 3.

3.2. Hypoxia effects

Applying the oxygen-dependent correction factor to the parameter combinations listed in Table 4 reproduced the direction of experimentally observed hypoxia effects, e.g. decreasing J_{Am}^{a} reduced total length, increased time until egg buffer mass reaches 0, and reduced survival. The best model of experimental hypoxia effects on *M. menidia* early life stages simultaneously had y_{VA} multiplied by c, and μ_{emb} and μ_{lar} divided by c (Fig. 4, Table 4, Figure S1). Although applying damage to y_{VA} alone affected all three state variables, concurrently increasing both mortality parameters improved the fit to the data (Table 4). The model in which the correction factor was applied to y_{VA}, μ_{emb}, and μ_{lar} also had the lowest AICc of all candidate models, with an AICc of 794.03 (AICc$_{min}$). Adding a correction factor to J_{M}^{v} simultaneously with these three parameters yielded a slightly higher AICc of 795.97 (Table 4). The ratio of Akaike weights shows that the model with c applied to y_{VA}, μ_{emb}, and μ_{lar}, is 2.67 times as likely as the one with c concurrently applied to J_{M}^{v} (Table 4). Applying a damage effect to maintenance was therefore not considered to have improved the fit. After estimating Z, we calculated the values of y_{VA}, μ_{emb}, and μ_{lar} when their respective correction factors are applied for each DO level (Table 5).

Interestingly, although J_{Am}^{a} affects the variables similarly to y_{VA}, the ratio of Akaike weights showed that the best fitting model is about 3000 times as likely as the version applying inhibition to J_{Am}^{a}, μ_{emb}, and μ_{lar} (Table 4). Reducing J_{Am}^{a} with hypoxia using the correction factor resulted in a visually good fit to the data across oxygen levels and variables. Simultaneously applying c to J_{Am}^{a} and both mortality parameters improved the fit compared to only applying it to J_{Am}^{a}, but this model fit

less well than the version that applied c to y_{VA}, μ_{emb}, and μ_{lar}, with an AICc value of 810.21 in the former model compared to 794.03 in the latter.

The estimated best value of Z, the parameter in the correction factor c, enables us to calculate that y_{VA} at the lowest oxygen level is 55 % of its value with no hypoxia stress. Reducing conversion efficiency alone produced small differences in survival at hatching because it prolongs the time spent in the embryo stage, which has a greater mortality rate than post-hatching in our model. Dividing both the pre- and post-hatching mortality rates by c more closely predicted the reduced survival rates in the low DO treatments, resulting in a best fitting model that explained observed hypoxia effects well by altering conversion efficiency, embryo mortality, and post-hatch mortality.

4. Discussion

By combining experimental data with unified principles for energetic allocation that are broadly applicable across species, we identified the conversion efficiency of assimilates into structure as the most likely process by which low oxygen levels affect early life stages of *M. menidia*. In comparing combinations of DEBkiss parameters that influence the ecological endpoints (total length, hatch timing, and survival), we discovered that applying correction factors based on damage production to the growth SU to reduce conversion efficiency (y_{VA}) and increase pre- and post-hatching mortality rates (μ_{emb} and μ_{lar}) best predicted the experimental effects of hypoxia on larval length, time to hatching, and early life survival. Through this model we have found evidence that the mechanism largely responsible for the observed hypoxia impacts on growth, hatch timing, and survival is the efficiency with which assimilated food or egg yolk is converted into structure. The limitations of this inference are discussed later.

Changes to assimilation in response to hypoxia have been recorded in other species, but the direction of that effect is species-dependent (reviewed in Thomas et al., 2019). In *M. menidia*, however, reducing assimilation with hypoxia rather than conversion efficiency yielded a
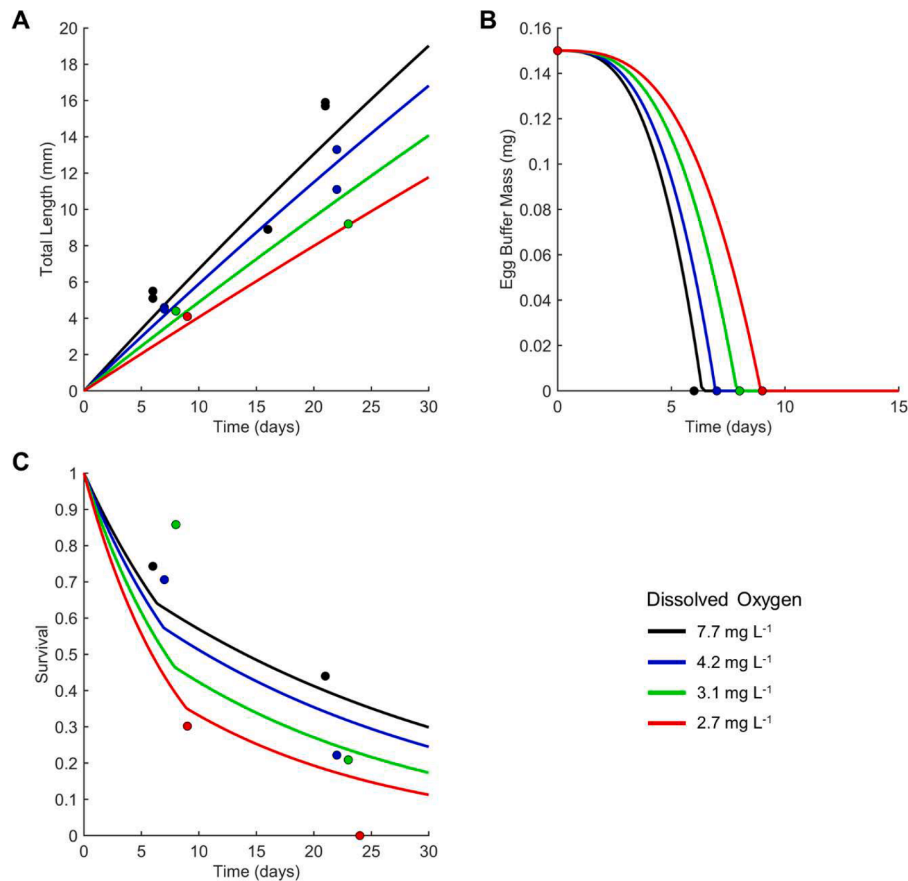
Fig. 4. Best fit of DEBkiss model to experimental data from four DO levels. The best fit of the predicted data (lines) to the observed data (dots) for four DO levels is shown, for early life data only. The best fitting model was selected based on lowest AICc. (A) is total length (mm) over time (days), (B) is egg buffer mass (mg) over time (days), and (C) is survival over time (days), with means rather than all data plotted for survival for ease of viewing. Full datasets used to estimate the correction factor parameter Z are plotted in Figure S1.

Table 5
Effects of correction factor c on parameters. The values of the DEBkiss parameters that best reproduce the hypoxia effects observed experimentally, calculated (with 95 % confidence intervals in brackets) for each DO treatment level using the correction factor c and the estimated value of $Z = 1.827$.

	Product of correction factor and initial parameter value			
	7.7 mg L^{-1}	4.2 mg L^{-1}	3.1 mg L^{-1}	2.7 mg L^{-1}
y_{VA}	0.333 [0.329, 0.339]	0.291 [0.284, 0.303]	0.240 [0.230, 0.257]	0.199 [0.188, 0.218]
μ_{emb}	0.0701 [0.0689, 0.0709]	0.0801 [0.0770, 0.0822]	0.0970 [0.0906, 0.101]	0.117 [0.107, 0.124]
μ_{lar}	0.0322 [0.0317, 0.0326]	0.0369 [0.0354, 0.0378]	0.0446 [0.0417, 0.0466]	0.0539 [0.0492, 0.0571]

worse fit despite the two parameters' similar contributions to the DEBkiss model in that both parameters are used to calculate predicted growth and egg buffer depletion. Reducing either assimilation or conversion efficiency would extend developmental time, which is consistent with previous work showing yolk absorption slows under hypoxia (Polymeropoulos et al., 2017). As maintenance costs must continue to be paid, this would increase the energy expended to produce each unit of structure (Kamler, 2008). Unlike assimilation, the mechanism for reduced conversion efficiency is most plausibly interpreted as damage to the synthesizing unit, perhaps from buildup of anaerobic byproducts, along with far less efficient ATP production through anaerobic respiration and slower rates of tissue differentiation (Bouma et al., 1994;

Kooijman, 2010a; Muller et al., 2019). The experimental DO levels are greater than the critical oxygen levels for oxygen-independent routine metabolism (P_{crit}) of 2.04 mg L^{-1} and 1.56 mg L^{-1} for embryos and 5dph larvae, respectively (Schwemmer, 2023). P_{crit} has been assumed by some to be the oxygen level at which anaerobic metabolism is triggered, but there is abundant evidence that some level of anaerobic metabolism can occur well above P_{crit} (Nonnotte et al., 1993; Maxime et al., 2000; Wood et al., 2018). Additional activity such as swimming bursts can drive up the need for anaerobiosis (Di Santo et al., 2017). Our evidence that conversion efficiency is reduced by hypoxia-induced damage suggests that anaerobic metabolism may be a mechanism of hypoxia effects in *M. menidia* early life stages even at oxygen levels above P_{crit}.

While y_{VA} is the best parameter to explain the hypoxia effects according to our model and AICc, it is nonetheless possible that J_{Am}^a is responsible for an unknown portion of the hypoxia effects. Because of near collinearity between J_{Am}^a and y_{VA}, our model does not allow us to test for the possibility that both parameters are simultaneously contributing to the observed hypoxia effects. It is not possible to simultaneously estimate both parameters, particularly when J_M is negligible as in the early life stages and J_{Am}^a and y_{VA} are directly multiplied to calculate growth in the model; we can adjust one or the other with the correction factor and get similar effects on the flux for growth with no way of determining which is correct. We therefore cannot test for partial contribution of the two parameters to hypoxia effects or quantify their relative contributions. If conversion efficiency were the only parameter varying across hypoxia treatments, one might expect all offspring to fully deplete the egg buffer and hatch at the same time, but with hatch size increasing with DO level. However, adjusting conversion efficiency with hypoxia does account for the observed significant

differences in hatch timing between DO treatments in *M. menidia* larvae (Cross et al., 2019) because y_{VA} reduces the body size at a given time, indirectly reducing the assimilation flux due to smaller body volume. Future work examining the effects of hypoxia on ingestion, defecation, respiration, and growth could help tease apart the relative contributions of y_{VA} and J_{Am}^a by allowing direct calculation of y_{VA}. Data on fecundity at different DO levels would provide information on the contribution of J_{Am}^a, although constant hypoxia through adulthood is unrealistic and this would assume the energy budget is impacted similarly across life stages.

Although both conversion efficiency and assimilation can explain hypoxia effects on total length and egg buffer mass over time, reducing them only produced a small decrease in survival relative to the data. Simultaneously applying *c* to both mortality rates better predicted the great reductions in survival at both hatching and 15 dph with hypoxia and improved the fit based on ΔAICc (Table 4). In the experiments, the lowest oxygen level (2.7 mg L^{-1}) had a mean hatch survival of 30.2 % while the mean survival in the other three treatments was over 70 % (Cross et al., 2019). By 15 dph fish from all three low oxygen treatments had lower survival than those from the normoxic treatment (Cross et al., 2019; Table 3). The additional mortality that was not accounted for by y_{VA} may have been related to unrepaired damage from buildup of toxic compounds during anaerobic metabolism (Richards, 2011). The mortality could also have resulted from failing to meet energetic demands with either aerobic or anaerobic metabolism (Richards, 2009) and, specifically in embryos, failure to reach a viable level of complexity before the yolk is depleted (Jager et al., 2013). Measurement of anaerobic byproducts such as lactate and morphometric assessment of dead embryos and larvae could help to identify the mechanisms underlying the mortality rates in future work. Although survival does not approach 0 % during the larval stage in our best fitting model (Fig. 4), all experimental replicates of the 2.7 mg L^{-1} DO treatment had 0 % survival by 15 dph, making larvae apparently more sensitive than embryos (Cross et al., 2019). The authors of the study attribute this to a possibly lower ability to suppress metabolism in larvae compared to embryos. While the increased mobility of larvae may allow aquatic surface respiration (Miller et al., 2016; Cross et al., 2019) and escape from hypoxia in a patchy and stratified estuarine environment, activity comes with elevated maintenance costs in addition to those required to begin feeding almost immediately after hatching (Middaugh and Lempesis, 1976). This may also be a crucial time to repair damage to the SU (Muller et al., 2019), and the combination of these additional maintenance demands may be too great to meet without restoration of normoxia. Though beyond the scope of this work, a model that captures stage-specific differences in maintenance costs and links them explicitly to survival may better capture the mechanism of high mortality in larvae.

Adding a correction factor to the volume-specific maintenance rate in addition to y_{VA}, μ_{emb}, and μ_{lar} did not substantially improve the fit according to AICc, suggesting that increasing maintenance costs is not an important bioenergetic mechanism underlying hypoxia response in early life stages. This is consistent with laboratory measurements showing no effect of these hypoxia levels on embryonic or larval metabolic rates (Schwemmer et al., 2020), but as noted earlier interpretation of respiration data is challenging and there was high individual variability in the data. In our model, egg buffer depletion is insensitive to changes in volume-specific maintenance costs, requiring a quadrupling to see a noticeable delay in hatching. Changing maintenance has much greater effects on length later in life while failing to explain differences in length at the time of hatching. Because maintenance is dependent on volume, it is a relatively small portion of the energy budget in the very small early life stages but increases substantially relative to the surface area-specific assimilation when larger sizes are reached, increasing its relative role in determining growth rate and, indirectly, all size-specific fluxes. Repairing damage and increasing ventilation and swimming activity could both increase maintenance costs (Thomas et al., 2019), but at the embryo stage very little activity is

possible. Some studies on fish responses to hypoxia suggest maintenance may drop temporarily due to the reduced capacity for aerobic metabolism at low DO levels, then subsequently be temporarily elevated after oxygen is restored because of recovery demands such as paying oxygen debt and removing or repairing damage from anaerobic byproducts (Heath and Pritchard, 1965; Claireaux and Chabot, 2016; Thomas et al., 2019). Such fluctuations in maintenance were not discernible in the time scale of our model, but future work should attempt to model the *M. menidia* early life energy budget during recovery from hypoxia.

Understanding the mechanisms of reduced growth and survival under hypoxia through DEB theory is useful for predicting life history effects, and although modeling population growth rates was not within the scope of this study, our results have implications for processes that influence fish population dynamics. The best fitting model predicts hypoxia-related reductions in long-term growth and survival that would certainly be detrimental to population growth under extended periods of low oxygen. Under this model, even restoring normoxia after 15 days would result in smaller size at age and survival rates than the control group, and damage to the SU is not reversed upon return to normoxia, but rather requires energy to repair (Muller et al., 2019). Delayed hatching and slower growth can lead to enhanced vulnerability to predation (Chambers and Leggett, 1987; Takasuka et al., 2007), further reducing fish survival rates beyond those observed in controlled laboratory conditions, although this is not always the case (Lankford et al., 2001; Robert et al., 2023). However, compensation of growth may be possible in aquatic ectotherms after exposure to hypoxia (Wei et al., 2008). An important assumption of our model is that several of the parameters have the same value across life stages (e.g. J_{Am}^a, J_M^v, y_{VA}) and similarly that values of the hypoxia correction factors are the same regardless of life stage. We lacked data on the effects of hypoxia on the proportion of total energy allocated to reproduction (1-κ), which is an additional component of DEB useful in connecting organismal effects to populations. Future experimentation could provide the adult-stage information that is needed to extend this DEB model to predict population growth, which would be useful for resource management applications (Kooijman et al., 2020; Lavaud et al., 2021), given the ecological importance of forage fishes and the value of model species like *M. menidia*.

The oxygen levels in the estuaries inhabited by *M. menidia* undergo great diel and seasonal fluctuations (Baumann et al., 2015). The effects of fluctuating DO cannot be resolved in the time scales used by our DEBkiss model, so we assumed constant DO levels. As a result, the model is more useful in identifying mechanisms than in quantitatively predicting how *M. menidia* will respond to realistic hypoxia scenarios, as lifelong constant hypoxia is unrealistic and this assumption may lead to overestimation of hypoxia effects. Studies comparing fish responses to static and fluctuating hypoxia treatments have suggested that fluctuations provided temporary relief and reduced sensitivity (Cross et al., 2019; Williams et al., 2019; Wang et al., 2021), although conflicting results also exist (Morrell and Gobler, 2020). It is also unrealistic for only a single environmental factor, in this case hypoxia, to influence the energy budget. Other studies have applied correction factors to DEB parameters to model other species' responses to hypoxia (Lavaud et al., 2019), seawater acidification (Jager et al., 2016; Moreira et al., 2022; Pousse et al., 2022) and pollutants (Muller et al., 2010; Desforges et al., 2017). The success of this approach with a wide variety of stressors makes it an ideal supplement to multistressor experiments, which are limited by logistical constraints. Modeling stressor effects with DEBkiss parameters can yield additional information about energetic mechanisms of responses and, with careful attention to the assumptions being made, may be useful in extrapolating stressor effects to additional magnitudes or combinations of stressors that would have been impractical to test experimentally, or to species with certain shared physiology or life history traits (Goussen et al., 2020; Boult and Evans, 2021). In the case of *M. menidia*, previous work showed that high CO_2 increases oxygen dependence of metabolism under both chronic (Schwemmer et al.,

2020) and acute hypoxia (Schwemmer, 2023). Adding oxygen as a second substrate in the SU would allow a DEB model to incorporate the oxygen limitation that is evidently induced by acidification.

Our best fitting model overestimated time to hatching at 7.7 mg L^{-1} DO and overestimated survival at age for the 2.7 and 4.2 mg L^{-1} treatments, which suggests there either may be a different nonlinear correction factor function that better fits the relationship between DO and the DEBkiss parameters or that there were additional factors contributing to these differences that the model does not account for. For example, hypoxia can reduce gonadosomatic index and gonad development in fish (Wu et al., 2003; Thomas et al., 2006; Landry et al., 2007), but we do not have data on gonad development or reproductive output after rearing *M. menidia* in hypoxia, which would allow us to investigate if κ is an affected parameter. Despite the potential for improvements with more data, the model was able to replicate the direction of effects and even account for some hypoxia effects in all three state variables simultaneously by changing only one parameter, either conversion efficiency or assimilation. Further, it provided these reasonable fits using an SU model based in well-studied and widely applicable Michaelis-Menten-Briggs-Haldane enzyme kinetics (Muller et al., 2019) rather than a more specialized or complex correction factor. While the generalized framework allows this model to be applied to other species, one species-specific assumption is that birth occurs at hatching. This is a fitting assumption for *M. menidia*, which are known to hatch with no detectable yolk (Bayliff, 1950) and begin feeding the day of hatching (Middaugh and Lempesis, 1976). However, investigators would need to alter the model or use different types of data before applying this approach to species that have an extended yolk-sac larval stage before feeding begins.

We end with a comment on the limitation of the "DEBtox" approach (Kooijman et al., 2009), a toxicology application of DEB from which DEBkiss stems, to identifying physiological modes of action in response to environmental stress. In Section 1 we cite the paper by Romoli et al. (2024) that highlighted the difficult modeling choices that are required. Here we chose to use DEBkiss coupled with several hypothesized responses to hypoxia. We selected the combination of DEB model and response hypothesis that best described given data (in an information theoretic sense using AICc), *conditional on the "correctness" of the model and of assumed values for some parameters*. Yet, for a case study in ecotoxicology, Romoli et al. showed that a different dominant physiological model of action was selected when using two different underlying DEB models that both give visually good fits to control data. Muller et al. (2010) demonstrated a related issue for a study of early life stage growth by identifying best fit submodel for larval growth of two closely related bivalve species exposed to mercury. Implausibly, the selected submodels were different to the extent that the best fit for one species was the worst for the other.

In the preceding discussion, we have offered a few suggestions for empirical work on whole organisms that would significantly help narrow down the DEB processes responsible for responses to hypoxia. However, it is likely that an additional, very promising way forward is to determine *suborganismal* processes co-occurring with the observed whole-organism responses. Transcriptomic data represent a particularly promising candidate (Murphy et al., 2018). We recognized this qualitatively in Section 2.4 and the Supplementary Materials when invoking genes controlling cell division and protein synthesis that are regulated by hypoxia-inducible factors. Stevenson et al. (2023) demonstrated the power of transcriptomic data in a study of killifish embryos exposed to a toxicant. The molecular data helped to identify damage mechanisms that in turn led to changes in DEB parameters. There are many further exciting possibilities for integrating suborganismal (molecular) data with DEBtox modeling.

5. Conclusions

With this simple and widely applicable DEBkiss model we were able

to attribute hypoxia-related variability in *M. menidia* growth, hatch timing, and survival to damage-induced reductions in conversion efficiency of assimilates into structure. Applying hypoxia corrections simultaneously to conversion efficiency and the mortality parameters for embryos and larvae provided the best fit, suggesting that hypoxia leads to both wasted energy and damage that cannot be sufficiently repaired in the early life stages. As lifelong, constant oxygen conditions are unrealistic in nature, the patterns modeled in this study should not be interpreted as a standalone prediction of what will happen to wild *M. menidia* populations as coastal hypoxia intensifies. Instead, this approach demonstrates the value of identifying energetic processes responsible for whole-organism effects of hypoxia to understand underlying energetic processes that are often time, labor, and cost-intensive to measure empirically, particularly in the early life stages, when biomass available for sampling is small and developmental changes are rapid. Through doing so we were able to support the utility of modeling inhibition and damage to synthesizing units and highlight conversion efficiency of food into growth as a primary mechanism by which hypoxia impacts an ecologically important forage fish and model species. Measuring suborganismal processes to identify physiological modes of action can refine this model so that it can better model this species' response to realistic hypoxia scenarios and, ultimately, how reductions in conversion efficiency could affect energy flow through food webs.

CRediT authorship contribution statement

Teresa G. Schwemmer: Writing – review & editing, Writing – original draft, Visualization, Methodology, Funding acquisition, Formal analysis, Data curation, Conceptualization. **Roger M. Nisbet:** Writing – review & editing, Writing – original draft, Methodology, Conceptualization. **Janet A. Nye:** Writing – review & editing, Funding acquisition, Conceptualization.

Declaration of competing interest

The authors declare that they have no known competing financial interests or personal relationships that could have appeared to influence the work reported in this paper.

Data availability

The datasets used for modeling can be found on BCO-DMO: early life total length, survival, and hatching: 10.1575/1912/bco-dmo.742200; early life total length with oxygen treatments: 10.1575/1912/bco-dmo.777130.1; hatching and survival with oxygen treatments: 10.1575/1912/bco-dmo.777117.1; total length of adults: 10.26008/1912/bco-dmo.845906.1; total length of larvae and juveniles: 10.1575/1912/bco-dmo.652124; egg production: 10.26008/1912/bco-dmo.845633.1. The BYOM and DEBkiss packages can be found at https://www.debtox.info/byom.html. The code for inputting data, parameter estimation, and plotting, for both the normoxic model and the model with hypoxia effects, can be found at github.com/tschwemmer/MenidiaDEB.

constructive and insightful feedback on this manuscript.

Supplementary materials

Supplementary material associated with this article can be found, in the online version, at doi:10.1016/j.ecolmodel.2024.110889.

References

AmP. 2023. Online database of DEB parameters, implied properties and referenced underlying data. www.bio.vu.nl/thb/deb/deblab/add_my_pet/ (accessed: 3 March 2023).

AmPtool, 2022. Software package, https://github.com/add-my-pet/AmPtool/.

Baumann, H., 2019. Experimental assessments of marine species sensitivities to ocean acidification and co-stressors: how far have we come? Can. J. Zool. 97, 399–408. dx. doi.org/10.1139/cjz-2018-0198.

Baumann, H., Smith, E.M., 2018. Quantifying metabolically driven pH and oxygen fluctuations in US nearshore habitats at diel to interannual time scales. Estuaries Coasts 41, 1102–1117. https://doi.org/10.1007/s12237-017-0321-3.

Baumann, H., Wallace, R.B., Tagliaferri, T., Gobler, C.J., 2015. Large natural pH, CO_2 and O_2 fluctuations in a temperate tidal salt marsh on diel, seasonal, and interannual time scales. Estuaries Coasts 38, 220–231. https://doi.org/10.1007/s12237-014-9800-y.

Bayliff, W.H., 1950. *The life history of the silverside* Menidia menidia *(Linnaeus)*. Chesapeake Bay Laboratory. State of Maryland Board of Natural Resources, Department of Research and Education, Solomons Island, Maryland.

Bengtson, D.A., 1984. Resource partitioning by *Menidia menidia* and *Menidia beryllina* (Osteichthyes: atherinidae). Mar. Ecol. Prog. Ser. 18, 21–30.

Bianchini, K., Wright, P.A., 2013. Hypoxia delays hematopoiesis: retention of embryonic hemoglobin and erythrocytes in larval rainbow trout, *Oncorhynchus mykiss*, during chronic hypoxia exposure. J. Exp. Biol. 216 (23), 4415–4425. https://doi.org/10.1242/jeb.083337.

Bigelow, H.B., Schroeder, W.C., 1953. *Fishes of the Gulf of Maine*. U.S. Fish and Wildlife Service. Fish. Bull. 53 (74), 577.

Boult, V.L., Evans, L.C., 2021. Mechanisms matter: predicting the ecological impacts of global change. Glob. Change Biol. 27 (9), 1689–1691. https://doi.org/10.1111/gcb.15527.

Bouma, T.J., De Visser, R., Janssen, J.H.J.A., De Kock, M.J., Van Leeuwen, P.H., Lambers, H, 1994. Respiratory energy requirements and rate of protein turnover in vivo determined by the use of an inhibitor of protein synthesis and a probe to assess its effect. Physiol. Plant. 92, 585–594. https://doi.org/10.1111/j.1399-3054.1994.tb03027.x.

Breitburg, D., Levin, L.A., Oschlies, A., et al., 2018. Declining oxygen in the global ocean and coastal waters. Science 359 (6371), eaam7240. https://doi.org/10.1126/science.aam7240.

Chambers, R.C., Leggett, W.C., 1987. Size and age at metamorphosis in marine fishes – an analysis of laboratory-reared winter flounder (*Pseudopleuronectes americanus*) with a review of variation in other species. Can. J. Fish. Aquat. Sci. 44 (11), 1936–1947. https://doi.org/10.1139/f87-238.

Chapman, L.J., McKenzie, D.J., 2009. Behavioral responses and ecological consequences. In: Richards, J.G., Farrell, A.P., Brauner, C.J. (Eds.), Fish Physiology, Vol. 27: Hypoxia. Academic Press, San Diego, pp. 25–77.

Claireaux, G., Chabot, D., 2016. Responses by fishes to environmental hypoxia: integration through Fry's concept of aerobic metabolic scope. J. Fish Biol. 88, 232–251. https://doi.org/10.1111/jfb.12833.

Concannon, C.A., Cross, E.L., Jones, L.F., Murray, C.S., Matassa, C.M., McBride, R.S., Baumann, H., 2021. Temperature-dependent effects on fecundity in a serial broadcast spawning fish after whole-life high CO_2 exposure. ICES J. Mar. Sci. 78 (10), 3724–3734. https://doi.org/10.1093/icesjms/fsab217.

Cross, E.L., Murray, C.S., Baumann, H., 2019. Diel and tidal pCO_2 x O_2 fluctuations provide physiological refuge to early life stages of a coastal forage fish. Sci. Rep. 9, 18146. https://doi.org/10.1038/s41598-019-53930-8.

Del Rio, A.M., Davis, B.E., Fangue, N.A., Todgham, A.E., 2019. Combined effects of warming and hypoxia on early life stage Chinook salmon physiology and development. Conserv. Physiol. 7 (1). https://doi.org/10.1093/conphys/coy078 coy078.

DePasquale, E., Baumann, H., Gobler, C.J., 2015. Vulnerability of early life stage Northwest Atlantic forage fish to ocean acidification and low oxygen. Mar. Ecol. Prog. Ser. 523, 145–156. https://doi.org/10.3354/meps11142.

Desforges, J.-P.W., Sonne, C., Dietz, R., 2017. Using energy budgets to combine ecology and toxicology in a mammalian sentinel species. Sci. Rep. 7, 46267. https://doi.org/10.1038/srep46267.

Di Santo, V., Kenaley, C.P., Lauder, G.V., 2017. High postural costs and anaerobic metabolism during swimming support the hypothesis of a U-shaped metabolism–speed curve in fishes. Proc. Nat. Acad. Sci. 114 (49), 13048–13053. https://doi.org/10.1073/pnas.1715141114.

Diaz, R.J., Rosenberg, R., 2008. Spreading dead zones and consequences for marine ecosystems. Science 321, 926–929. https://doi.org/10.1126/science.1156401.

Evans, M.R., Grimm, V., Johst, K., et al., 2013. Do simple models lead to generality in ecology? Trends Ecol. Evol. (Amst.) 28 (10), 578–583. https://doi.org/10.1016/j.tree.2013.05.022.

Farrell, A.P., Brauner, C.J., 2009. Fish Physiology, 27. Hypoxia. Academic Press, London.

Goussen, B., Rendal, C., Sheffield, D., Butler, E., Price, O.R., Ashauer, R., 2020. Bioenergetics modelling to analyze and predict the joint effects of multiple stressors: meta-analysis and model corroboration. Sci. Total. Environ. 749, 141509. https://doi.org/10.1016/j.scitotenv.2020.141509.

Grear, J.S., O'Leary, C.A., Nye, J.A., Tettelbach, S.T., Gobler, C.J, 2020. Effects of coastal acidification on North Atlantic bivalves: interpreting laboratory responses in the context of *in situ* populations. Mar. Ecol. Prog. Ser. 633, 89–104. https://doi.org/10.3354/meps13140.

Gruber, J., 2011. Warming up, turning sour, losing breath: ocean biogeochemistry under global change. Phil. Trans. R. Soc. A 369, 1980–1996. https://doi.org/10.1098/rsta.2011.0003.

Hamda, N.T., Martin, B., Poletto, J.B., Cocherell, D.E., Fangue, N.A., Van Eenennaam, J., Mora, E.A., Danner, E., 2019. Applying a simplified energy-budget model to explore the effects of temperature and food availability on the life history of green sturgeon (*Acipenser medirostris*). Ecol. Modell. 395, 1–10. https://doi.org/10.1016/j.ecolmodel.2019.01.005.

Heath, A.G., Pritchard, A.W., 1965. Effects of severe hypoxia on carbohydrate energy stores and metabolism in two species of fresh-water fish. Physiol. Zool. 38 (4), 325–334. https://doi.org/10.1086/physzool.38.4.30152409.

Holling, C.S., 1966. The strategy of building models of complex ecological systems. In: Watt, K.E.F. (Ed.), Systems Analysis in Ecology. Academic Press, pp. 195–214.

Jager, T. 2018. DEBkiss: A Simple Framework for Animal Energy Budgets. Version 2.0. Leanpub: https://leanpub.com/debkiss_book.

Jager, T., Martin, B.T., Zimmer, E.I., 2013. DEBkiss or the quest for the simplest generic model of animal life history. J. Theor. Biol. 328, 9–18. https://doi.org/10.1016/j.jtbi.2013.03.011.

Jager, T., Ravagnan, E., Dupont, S., 2016. Near-future ocean acidification impacts maintenance costs in sea-urchin larvae: identification of stress factors and tipping points using a DEB modelling approach. J. Exp. Mar. Biol. Ecol. 474, 11–17. https://doi.org/10.1016/j.jembe.2015.09.016.

Jager, T., Nepstad, R., Hansen, B.H., Farkas, J., 2018. Simple energy-budget model for yolk-feeding stages of Atlantic cod (*Gadus morhua*). Ecol. Modell. 385, 213–219. https://doi.org/10.1016/j.ecolmodel.2018.08.003.

Jager, T., Malzahn, A.M., Hagemann, A., Hansen, B.H., 2022. Testing a simple energy-budget model for yolk-feeding stages of cleaner fish. Ecol. Modell. 469, 110005. https://doi.org/10.1016/j.ecolmodel.2022.110005.

Jusup, M., Sousa, T., Domingos, T., Labinac, V., Marn, N., Wang, Z., Klanjšček, T., 2017. Physics of metabolic organization. Phys. Life Rev. 20, 1–39. https://doi.org/10.1016/j.plrev.2016.09.001.

Kamler, E., 2008. Resource allocation in yolk-feeding fish. Rev. Fish. Biol. Fisheries 18, 143–200. https://doi.org/10.1007/s11160-007-9070-x.

Klahre, L.E., 1997. Countergradient Variation in Egg Production Rate of the Atlantic Silverside *Menidia menidia*. Stony Brook University. Master's Thesis.

Kooijman, S.A.L.M., 1998. The Synthesizing Unit as model for the stoichiometric fusion and branching of metabolic fluxes. Biophys. Chem. 73, 179–188. https://doi.org/10.1016/S0301-4622(98)00162-8.

Kooijman, S.A.L.M., 2010a. Dynamic Energy Budget Theory for Metabolic Organisation. Cambridge University Press, Cambridge.

Kooijman, S.A.L.M., 2010b. Comments On Dynamic Energy Budget Theory For Metabolic Organisation. Cambridge University Press, Cambridge.

Kooijman, S.A.L.M., 2018. Models in stress research. Ecol. Complex. 34, 161–177. https://doi.org/10.1016/j.ecocom.2017.07.006.

Kooijman, S.A.L.M., Metz, J.A.J., 1984. On the dynamics of chemically stressed populations: the deduction of population consequences from effects on individuals. Ecotoxicol. Environ. Saf. 8 (3), 254–274. https://doi.org/10.1016/0147-6513(84)90029-0.

Kooijman, S.A.L.M., Baas, J., Bontje, D., Broerse, M., van Gestel, C.A.M., Jager, T., 2009. Ecotoxicological applications of dynamic energy budget theory. In: Devillers, J. (Ed.), Emerging Topics in Ecotoxicology, Vol. 2: Ecotoxicology Modeling. Springer, Boston, MA, pp. 237–259. https://doi.org/10.1007/978-1-4419-0197-2_9.

Kooijman, S.A.L.M., Lika, K., Augustine, S., Marn, N., Kooi, B.W., 2020. The energetic basis of population growth in animal kingdom. Ecol. Modell. 428, 109055. https://doi.org/10.1016/j.ecolmodel.2020.109055.

Landry, C.A., Steele, S.L., Manning, S., Cheek, A.O., 2007. Long term hypoxia suppresses reproductive capacity in the estuarine fish, *Fundulus grandis*. Comp. Biochem. Physiol. Part A Mol. Integr. Physiol. 148 (2), 317–323. https://doi.org/10.1016/j.cbpa.2007.04.023.

Lankford, T.E., Billerbeck, J.M., Conover, D.O., 2001. Evolution of intrinsic growth and energy acquisition rates. II. Trade-offs with vulnerability to predation in *Menidia menidia*. Evolution (N Y) 55 (9), 1873–1881. https://doi.org/10.1111/j.0014-3820.2001.tb00836.x.

Lavaud, R., Filgueira, R., Augustine, S, 2019. The role of Dynamic Energy Budgets in conservation physiology. Conserv. Physiol. 9 (1). https://doi.org/10.1093/conphys/coab083 coab083.

Lavaud, R., Filgueira, R., Augustine, S, 2021. The role of Dynamic Energy Budgets in conservation physiology. Conserv. Physiol. 9 (1). https://doi.org/10.1093/conphys/coab083 coab083.

Letcher, B.H., Bengtson, D.A., 1993. Effects of food density and temperature on feeding and growth of young inland silversides (*Menidia beryllina*). J. Fish Biol. 43, 671–686. https://doi.org/10.1111/j.1095-8649.1993.tb01145.x.

Lika, K., Kearney, M.R., Freitas, V., van der Veer, H.W., van der Meer, J., Mijsman, J.W. M., Pecqueries, L., Kooijman, S.A.L.M., 2011. The "covariation method" for estimating the parameters of the standard Dynamic Energy Budget model I: philosophy and approach. J. Sea Res. 66 (4), 270–277. https://doi.org/10.1016/j.seares.2011.07.010.

Marques, G.M., Augustine, S., Lika, K., Pecquerie, L., Domingos, T., Kooijman, S.A.L.M, 2018. The AmP project: comparing species on the basis of dynamic energy budget parameters. PLoS Comput. Biol. 14 (5). https://doi.org/10.1371/journal.pcbi.1006100 e1006100.

Martin, B.T., Jager, T., Nisbet, R.M., Preuss, T.G., Grimm, V., 2013. Predicting population dynamics from the properties of individuals: a cross-level test of Dynamic Energy Budget theory. Am. Nat. 181 (4), 506–519. https://doi.org/10.1086/669904.

Martin, B.T., Heintz, R., Danner, E.M., Nisbet, R.M., 2017. Integrating lipid storage into general representations of fish energetics. J. Anim. Ecol 86, 812–825. https://doi.org/10.1111/1365-2656.12667.

Maxime, V., Pichavant, K., Boeuf, G., Nonnotte, G., 2000. Effects of hypoxia on respiratory physiology of turbot, *Scophthalmus maximus*. Fish Physiol. Biochem. 22, 51–59. https://doi.org/10.1023/A:1007829214826.

Middaugh, D.P., 1981. Reproductive ecology and spawning periodicity of the atlantic silverside, *Menidia menidia* (Pisces: Atherinidae). Copeia 1981 (4), 766–776. https://doi.org/10.2307/1444176.

Middaugh, D.P., Lempesis, P.W., 1976. Laboratory spawning and rearing of a marine fish, the silverside *Menidia menidia menidia*. Mar. Biol. 35, 295–300. https://doi.org/10.1007/BF00386640.

Middaugh, D.P., Hemmer, M.J., 1992. Reproductive ecology of the inland silverside, *Menidia beryllina*, (Pisces: Atherinidae) from Blackwater Bay, Florida. Copeia 1992 (1), 53–61. https://doi.org/10.2307/1446535.

Miller, S.H., Breitburg, D.L., Burrell, R.B., Keppel, A.G., 2016. Acidification increases sensitivity to hypoxia in important forage fishes. Mar. Ecol. Prog. Ser. 549, 1–8. https://doi.org/10.3354/meps11695.

Moreira, J.M., Candeias Mendes, A., Maulvault, A.L., Marques, A., Rosa, R., Pousão-Ferreira, P., Sousa, T., Anacleto, P., Marques, G.M, 2022. Impacts of ocean warming and acidification on the energy budget of three commercially important fish species. Conserv. Physiol. 10 (1). https://doi.org/10.1093/conphys/coac048 coac048.

Morrell, B.K., Gobler, C.J., 2020. Negative effects of diurnal changes in acidification and hypoxia on early-life stage estuarine fishes. Diversity (Basel) 12, 25. https://doi.org/10.3390/d12010025.

Muller, E.B., Nisbet, R.M., Berkley, H.A., 2010. Sublethal toxicant effects with dynamic energy budget theory: model formulation. Ecotoxicology 19, 48–60. https://doi.org/10.1007/s10646-009-0385-3.

Muller, E.B., Klanjšček, T., Nisbet, R.M., 2019. Inhibition and damage schemes within the synthesizing unit concept of dynamic energy budget theory. J. Sea Res. 143, 165–172. https://doi.org/10.1016/j.seares.2018.05.006.

Murphy, C.A., Nisbet, R.M., Antczak, P., Garcia-Reyero, N., Gergs, A., Lika, K., Mathews, T., Muller, E.B., Nacci, D., Peace, A., Remien, C.H., Schultz, I.R., Stevenson, L.M., Watanabe, K.H., 2018. Incorporating suborganismal processes into Dynamic Energy Budget models for ecological risk assessment. Integr. Environ. Assess. Manag. 14 (5), 615–624. https://doi.org/10.1002/ieam.4063.

Murray, C.S., Baumann, H., 2018a. You Better Repeat It: complex CO₂ × Temperature Effects in Atlantic Silverside Offspring Revealed by Serial Experimentation. Diversity (Basel) 10, 69. https://doi.org/10.3390/d10030069.

Murray, C.S., Baumann, H., 2020. Are long-term growth responses to elevated *p*CO₂ sex-specific in fish? PLoS ONE 15 (7), e0235817. https://doi.org/10.1371/journal.pone.0235817.

Murray, C.S., Fuiman, L.A., Baumann, H., 2017. Consequences of elevated CO₂ exposure across multiple life stages in a coastal forage fish. ICES J. Mar. Sci. 74 (4), 1051–1061. https://doi.org/10.1093/icesjms/fsw179.

Niklitschek, E.J., Secor, D.H., 2005. Modeling spatial and temporal variation of suitable nursery habitats for Atlantic sturgeon in the Chesapeake Bay. Estuar. Coast. Shelf Sci. 64, 135–148. https://doi.org/10.1016/j.ecss.2005.02.012.

Nisbet, R.M., Gurney, W.S.C., Murdoch, W.W., McCauley, E., 1989. Structured population models: a tool for linking effects at individual and population level. Biol. J. Linn. Soc. 37, 79–99. https://doi.org/10.1111/j.1095-8312.1989.tb02006.x.

Nisbet, R.M., Muller, E.B., Lika, K., Kooijman, S.A.L.M., 2000. From molecules to ecosystems through dynamic energy budget models. J. Anim. Ecol. 69, 913–926.

Nonnotte, G., Maxime, V., Truchot, J.P., Williot, P., Peyraud, C., 1993. Respiratory responses to progressive ambient hypoxia in the sturgeon, *Acipenser baeri*. Respir. Physiol. 91, 71–82. https://doi.org/10.1016/0034-5687(93)90090-W.

O'Donnell, J., Dam, H.G., Bohlen, W.F., Fitzgerald, W., Gay, P.S., Houk, A.E., Cohen, D. C., Howard-Strobel, M.M., 2008. Intermittent ventilation in the hypoxic zone of western Long Island Sound during the summer of 2004. J. Geophys. Res. 113, C09025. https://doi.org/10.1029/2007JC004716.

Polymeropoulos, E.T., Elliott, N.G., Frappell, P.B., 2017. Hypoxic acclimation leads to metabolic compensation after reoxygenation in Atlantic salmon yolk-sac alevins. Comp. Biochem. Physiol. A 213, 28–35. https://doi.org/10.1016/j.cbpa.2017.08.011.

Pousse, É., Munroe, D., Hart, D., Hennen, D., Cameron, L.P., Rheuban, J.E., Wang, Z.A., Wikfors, G.H., Meseck, S.L., 2022. Dynamic energy budget modeling of Atlantic surfclam, *Spisula solidissima*, under future ocean acidification and warming. Mar. Environ. Res. 177, 105602. https://doi.org/10.1016/j.marenvres.2022.105602.

Richards, J.G., 2009. Metabolic and molecular responses of fish to hypoxia. In: Richards, J.G., Farrell, A.P., Brauner, C.J. (Eds.), Fish Physiology, Vol. 27: Hypoxia. Academic Press, San Diego, pp. 443–485.

Richards, J.G., 2011. Physiological, behavioral and biochemical adaptations of intertidal fishes to hypoxia. J. Exp. Biol. 214, 191–199. https://doi.org/10.1242/jeb.047951.

Robert, D., Shoji, J., Sirois, P., Takasuka, A., Catalán, I.A., et al., 2023. Life in the fast lane: revisiting the fast growth—High survival paradigm during the early life stages of fish. Fish Fish. 24, 863–888. https://doi.org/10.1111/faf.12774.

Rombough, P.J., 1988. Respiratory gas exchange, aerobic metabolism, and effects of hypoxia during early life. In: Hoar, W.S., Randall, D.J. (Eds.), Fish Physiology, Vol. 11: The Physiology of Developing Fish, Part A: Eggs and Larvae. Academic Press, San Diego, pp. 59–162.

Romoli, C., Jager, T., Trijau, M., Goussen, B., Gergs, A., 2024. Environmental risk assessment with energy budget models: a comparison between two models of different complexity. Environ. Toxicol. Chem. 43 (2), 440–449. https://doi.org/10.1002/etc.5795.

Schwemmer, T.G., 2023. Early Life Physiological and Energetic Responses of Atlantic Silversides (*Menidia menidia*) to Ocean Acidification, Warming, and Hypoxia. Doctoral dissertation. ProQuest Dissertations Publishing. State University of New York at Stony Brook, Stony Brook, NY.

Schwemmer, T.G., Baumann, H., Murray, C.S., Molina, A.I., Nye, J.A., 2020. Acidification and hypoxia interactively affect metabolism in embryos, but not larvae, of the coastal forage fish *Menidia menidia*. J. Exp. Biol. 223, jeb228015. https://doi.org/10.1242/jeb.228015.

Sibly, R.M., Grimm, V., Martin, B.T., Johnston, A.S.A., et al., 2013. Representing the acquisition and use of energy by individuals in agent-based models of animal populations. Methods Ecol. Evol. 4, 151–161. https://doi.org/10.1111/2041-210x.12002.

Smallegange, I.M., Caswell, H., Toorians, M.E.M., de Roos, A.M., 2017. Mechanistic description of population dynamics using dynamic energy budget theory incorporated into integral projection models. Methods Ecol. Evol. 8, 146–154. https://doi.org/10.1111/2041-210X.12675.

Stevenson, L.M., Muller, E.B., Nacci, D., Clark, B.W., Whitehead, A., Nisbet, R.M., 2023. Connecting suborganismal data to bioenergetic processes: killifish embryos exposed to a dioxin-like compound. Environ. Toxicol. Chem. 42 (9), 2040–2053. https://doi.org/10.1002/etc.5680.

Stierhoff, K.L., Targett, T.E., Miller, K., 2006. Ecophysiological responses of juvenile summer and winter flounder to hypoxia: experimental and modeling analyses of effects on estuarine nursery quality. Mar. Ecol. Prog. Ser. 325, 255–266. https://doi.org/10.3354/meps325255.

Stierhoff, K.L., Targett, T.E., Power, J.H., 2009. Hypoxia-induced growth limitation of juvenile fishes in an estuarine nursery: assessment of small-scale temporal dynamics using RNA:DNA. Can. J. Fish. Aquat. Sci. 66 (7), 1033–1047. https://doi.org/10.1139/F09-066.

Tai, T.C., Sumaila, U.R., Cheung, W.W.L., 2021. Ocean acidification amplifies multi-stressor impacts on global marine invertebrate fisheries. Front. Mar. Sci. 8, 596644. https://doi.org/10.3389/fmars.2021.596644.

Takasuka, A., Aoki, I., Oozeki, Y., 2007. Predator-specific growth-selective predation on larval Japanese anchovy *Engraulis japonicus*. Mar. Ecol. Prog. Ser. 350, 99–107. https://doi.org/10.3354/meps07158.

Taylor, J.C., Miller, J.M., 2001. Physiological performance of juvenile southern flounder, *Paralichthys lethostigma* (Jordan and Gilbert, 1884), in chronic and episodic hypoxia. J. Exp. Mar. Biol. Ecol. 258, 195–214. https://doi.org/10.1016/S0022-0981(01)00215-5.

Testa, J.M., Murphy, R.R., Brady, D.C., Kemp, W.M., 2018. Nutrient- and climate-induced shifts in the phenology of linked biogeochemical cycles in a temperate estuary. Front. Mar. Sci. 5, 114. https://doi.org/10.3389/fmars.2018.00114.

Thomas, P., Rahman, M.S., Kummer, J.A., Lawson, S, 2006. Reproductive endocrine dysfunction in Atlantic croaker exposed to hypoxia. Mar. Environ. Res. 62, S249–S252. https://doi.org/10.1016/j.marenvres.2006.04.031.

Thomas, Y., Flye-Sainte-Marie, J., Chabot, D., Aguirre-Velarde, A., Marques, G.M., Pecquerie, Laure., 2019. Effects of hypoxia on metabolic functions in marine organisms: observed patterns and modelling assumptions within the context of Dynamic Energy Budget (DEB) theory. J. Sea Res. 143, 231–242. https://doi.org/10.1016/j.seares.2018.05.001.

Vanderplancke, G., Claireaux, G., Quazuguel, P., Madec, L., Ferraresso, S., Sévère, A., Zambonino-Infante, J.-L., Mazurais, D., 2015. Hypoxic episode during the larval period has long-term effects on European sea bass juveniles (*Dicentrarchus labrax*). Mar. Biol. 162, 367–376. https://doi.org/10.1007/s00227-014-2601-9.

Wagenmakers, E.-J., Farrell, S., 2004. AIC model selection using Akaike weights. Psychon. Bull. Rev. 11 (1), 192–196. https://doi.org/10.3758/BF03206482.

Wang, J., Yang, Y., Wang, Z., Xu, K., Xiao, X., Mu, W., 2021. Comparison of effects in sustained and diel-cycling hypoxia on hypoxia tolerance, histology, physiology, and expression of clock genes in high latitude fish *Phoxinus lagowskii*. Comp. Biochem. Physiol. A Mol. Integr. Physiol. 260, 111020. https://doi.org/10.1016/j.cbpa.2021.111020.

Wei, L.-Z., Zhang, X.-M., Li, J., Huang, G.-Q., 2008. Compensatory growth of Chinese shrimp, *Fenneropenaeus chinensis* following hypoxic exposure. Aquacult. Int. 16, 455–470. https://doi.org/10.1007/s10499-007-9158-2.

Williams, K.J., Cassidy, A.A., Verhille, C.E., Lamarre, S.G., MacCormack, T.J., 2019. Diel cycling hypoxia enhances hypoxia tolerance in rainbow trout (*Oncorhynchus mykiss*): evidence of physiological and metabolic plasticity. J. Exp. Biol. 222 (14), jeb206045. https://doi.org/10.1242/jeb.206045.

Wood, C.M., 2018. The fallacy of the P_{crit} – are there more useful alternatives? J. Exp. Biol. 221, jeb163717. https://doi.org/10.1242/jeb.163717.

Wu, R.S.S., Zhou, B.S., Randall, D.J., Woo, N.Y.S., Lam, P.K.S., 2003. Aquatic hypoxia is an endocrine disruptor and impairs fish reproduction. Environ. Sci. Technol. 37 (6), 1137–1141. https://doi.org/10.1021/es0258327.

Zambonino-Infante, J.L., Mazurais, D., Dubuc, A., Quéau, P., Vanderplancke, G., Servili, A., Cahu, C., Le Bayon, N., Huelvan, C., Claireaux, G., 2017. An early life hypoxia event has a long-term impact on protein digestion and growth in juvenile European sea bass. J. Exp. Biol. 220 (10), 1846–1851. https://doi.org/10.1242/jeb.154922.

Zhu, C.-D., Wang, Z.-H., Yan, B, 2013. Strategies for hypoxia adaptation in fish species: a review. J. Comp. Physiol. B 183, 1005–1013. https://doi.org/10.1007/s00360-013-0762-3.